

## Granulocyte Colony-Stimulating Factor Induces Osteoblast Apoptosis and Inhibits Osteoblast Differentiation

Matthew J Christopher and Daniel C Link

**ABSTRACT:** Long-term treatment of mice or humans with granulocyte colony-stimulating factor (G-CSF) is associated with a clinically significant osteopenia characterized by increased osteoclast activity and number. In addition, recent reports have observed a decrease in number of mature osteoblasts during G-CSF administration. However, neither the extent of G-CSF's suppressive effect on the osteoblast compartment nor its mechanisms are well understood. Herein, we show that short-term G-CSF treatment in mice leads to decreased numbers of endosteal and trabecular osteoblasts. The effect is specific to mature osteoblasts, because bone-lining cells, osteocytes, and periosteal osteoblasts are unaffected. G-CSF treatment accelerates osteoblast turnover in the bone marrow by inducing osteoblast apoptosis. In addition, whereas G-CSF treatment sharply increases osteoprogenitor number, differentiation of mature osteoblasts is impaired. Bone marrow transplantation studies show that G-CSF acts through a hematopoietic intermediary to suppress osteoblasts. Finally, G-CSF treatment, through suppression of mature osteoblasts, also leads to a marked decrease in osteoprotegerin expression in the bone marrow, whereas expression of RANKL remains relatively constant, suggesting a novel mechanism contributing to the increased osteoclastogenesis seen with long-term G-CSF treatment. In sum, these findings suggest that the hematopoietic system may play a novel role in regulating osteoblast differentiation and apoptosis during G-CSF treatment.

**J Bone Miner Res 2008;23:1765–1774. Published online on June 30, 2008; doi: 10.1359/JBMR.080612**

**Key words:** osteoblasts, osteoclasts, cytokines

### INTRODUCTION

BONE MARROW IS the normal site of both hematopoiesis and bone metabolism. As predicted by their proximity, regulation of these tissues is highly integrated. There is strong evidence that osteoblasts play a key role in establishing and maintaining an appropriate microenvironment for hematopoietic stem cells. Conversely, the hematopoietic compartment is also known to regulate bone metabolism, largely through the production of hematopoietic cytokines.<sup>(1,2)</sup>

Granulocyte-colony stimulating factor (G-CSF) is the principal cytokine regulating granulopoiesis. Long-term treatment with G-CSF is associated with development of clinically significant osteopenia, characterized by decreased BMD and vertebral compression fractures.<sup>(3,4)</sup> In a recent study, the incidence of osteopenia in patients with severe congenital neutropenia (SCN) treated chronically with G-CSF was 28%.<sup>(5)</sup> Similarly, long-term exposure to G-CSF in mice leads to a decrease in cortical and trabecular bone, suggesting that it is G-CSF and not the underlying disease that is causing osteopenia in patients with SCN.<sup>(4,5)</sup>

There is evidence that G-CSF induces osteopenia in part by stimulating osteoclast activity. G-CSF treatment in-

creases osteoclast number in treated mice and increases the level of urine deoxypyridinoline in humans.<sup>(6)</sup> Several potential mechanisms by which G-CSF stimulates osteoclastogenesis have been advanced. G-CSF increases the proliferation of myeloid progenitors, potentially increasing the pool of monocytic precursors from which osteoclasts derive.<sup>(7)</sup> In addition, G-CSF has been shown directly to augment osteoclast formation and activity *in vitro*.<sup>(8)</sup> Nevertheless, the mechanisms by which G-CSF stimulates osteoclastogenesis *in vivo* remain undefined.

Whereas long-term G-CSF treatment results in increased osteoclastogenesis, recent evidence suggests that short-term G-CSF administration decreases osteoblast number and activity.<sup>(6,9,10)</sup> Our laboratory has shown that administration of G-CSF for 5 days in mice results in a marked decrease in histologically identifiable osteoblasts along bone surfaces and a corresponding decrease in osteocalcin mRNA.<sup>(10)</sup> Whether this decrease in osteoblast number results from increased osteoblast turnover or from a defect in osteoblast development remains unclear. A third possibility—that G-CSF induces osteoblast quiescence—was raised in a recent report by Katayama et al.,<sup>(9)</sup> who observed a preponderance of bone lining cells in G-CSF-treated mice.

In this study, we use transgenic mice expressing the green fluorescent protein (GFP) under control of an osteoblast lineage-specific promoter (pOBCol2.3-GFP mice) to measure osteoblast turnover during G-CSF administration. We show that G-CSF administration leads to a selective

---

The authors state that they have no conflicts of interest.

---

Division of Oncology, Department of Medicine, Washington University School of Medicine, St Louis, Missouri, USA.

reduction in number of mature endosteal and trabecular osteoblasts that is secondary to both an increase in osteoblast apoptosis and inhibition of osteoblast differentiation. Bone marrow transplantation studies show that G-CSF regulates osteoblasts indirectly, through a hematopoietic intermediary. Finally, we show that G-CSF treatment markedly decreases the bone marrow expression of osteoprotegerin (OPG), providing a novel mechanism by which G-CSF activates osteoclasts.

## MATERIALS AND METHODS

### *Mice*

The generation and characterization of pOBCol2.3-GFP mice, kindly provided by David Rowe at the University of Connecticut, have been described elsewhere.<sup>(11)</sup> Mice were maintained in a pathogen-free barrier facility in accordance with Washington University Animal Studies Committee guidelines. Six- to 12-wk-old age- and sex-matched mice were used in all studies. G-CSF receptor (G-CSFR)-deficient mice backcrossed onto a C57BL/6 background were generated, as previously described.<sup>(12)</sup>

### *G-CSF administration*

Recombinant human G-CSF, a generous gift from Amgen, was diluted in PBS with 0.1% low endotoxin BSA (Sigma) and administered by twice daily subcutaneous injection at a dose of 250  $\mu\text{g}/\text{kg}/\text{d}$  for the length of time indicated.

### *Immunohistochemistry and histomorphometry*

Long bones from pOBCol2.3-GFP and wildtype mice were processed as previously described.<sup>(10)</sup> Briefly, femurs and tibias were harvested, fixed overnight in 10% neutral formalin, decalcified by incubating in 14% EDTA at 4°C for 7–10 days, and embedded in paraffin. Paraffin-embedded sections were deparaffinized and rehydrated, and antigen retrieval was performed by soaking sections in DeCal Retrieval Solution (Biogenex) per the manufacturer's instructions. GFP expression was assessed using a rabbit anti-GFP polyclonal antibody (Chemicon International), and positive cells were visualized using Vector Elite ABC kit and DAB substrate (Vector Laboratories) with Nuclear Fast Red counterstain (Sigma). Slides were analyzed in a blinded fashion to determine the number of osteoblasts per millimeter bone perimeter, osteoblast surface percent, bone-lining cell surface percent, and osteocyte number per trabecular area. Bone lining cells and osteoblasts were differentiated based on morphology. Analysis was confined to the trabecular metaphyseal region distal to the growth plate. Osteoclasts were identified by staining sections for TRACP. Osteoclast number and osteoclast surface were calculated based on the presence of TRACP<sup>+</sup> cells on trabecular surfaces.

Osteoid surface was determined by analyzing undecalcified, methyl methacrylate-embedded sections stained using

the Masson trichrome technique. To determine mineralization rate, mice were injected twice with 0.5 mg calcein (Sigma) before and after 7 day G-CSF treatment. Forty-eight hours after the second injection, calvaria were harvested, fixed in 70% ethanol, and embedded in methyl methacrylate. Mineral apposition rate and mineralizing surface were analyzed by fluorescent microscopy, as previously described.<sup>(13)</sup> Images were acquired with Nikon microphot SA microscope using Nikon plan  $\times 10$  and  $\times 20$  objectives (Nikon Instruments) and a digital camera from Colorview Soft Imaging System. All parameters were analyzed using OsteoMeasure Histomorphometry System (OsteoMetrics).

### *Osteocalcin RNA in situ*

Osteocalcin sense and antisense <sup>33</sup>P-labeled probes for RNA in situ were generated using a SP6/T7 Transcription Kit (Roche) using a plasmid generously provided by David Ornitz (Washington University). RNA in situ hybridization was performed as previously described.<sup>(14)</sup>

### *Real-time quantitative RT-PCR*

Femurs were flushed with 1 ml of TRIzol reagent (Invitrogen), and RNA was isolated according to the manufacturer's instructions. Real-time RT-PCR was performed as previously described.<sup>(10)</sup> Primer sequences and annealing conditions are available on request.

### *Isolation of osteoblast lineage cells by flow cytometry*

Bone marrow cells were recovered from the femurs of pOBCol2.3-GFP mice by flushing with PBS. The femurs were infused with PBS containing 50 mg/ml type II collagenase (Worthington Biochemical) and incubated at 37°C for 15 min. The collagenase-treated femurs were flushed again with PBS, cells were pooled, and the process was repeated for a total six digests. Pilot experiments showed that virtually all recoverable GFP<sup>+</sup> cells were found in these six digests (data not shown).

To quantify osteoblast lineage cells, pooled fractions were stained with allophycocyanin (APC)-conjugated anti-mouse CD45 and phycoerythrin (PE) conjugated anti-mouse Ter119 antibodies (eBiosciences). CD45<sup>-</sup>, Ter119<sup>-</sup>, GFP<sup>+</sup> cells were enumerated on a FACScan flow cytometer (Becton Dickinson). In some experiments, CD45<sup>-</sup>, Ter119<sup>-</sup>, GFP<sup>+</sup> cells were sorted using a MoFlo high-speed cell sorter (Dako).

### *BrdU labeling*

pOBCol2.3-GFP mice were treated with 2 mg BrdU (Sigma) daily for 14 days before G-CSF treatment. In a separate study, mice were given 2 mg of BrdU twice daily for 5 days after G-CSF treatment. Cell fractions containing osteoblasts were isolated as described and stained with PE-conjugated anti-Ter119 and biotinylated anti-CD45 coupled with Alexa 750-conjugated streptavidin (Invitro-

gen). BrdU positivity was assessed using the BD Pharmingen BrdU Flow Kit (Becton Dickinson) and an Alexa 647-conjugated anti-BrdU antibody (Invitrogen).

#### *Activated caspase 3 analysis*

Bone marrow cells harvested from pOBCOL2.3-GFP mice were stained with APC-conjugated anti-mouse Ter119 and biotinylated anti-mouse CD45 (eBiosciences) coupled with Alexa 750-conjugated streptavidin (Invitrogen). Cells were fixed and permeabilized with BD Cytotfix/Cytoperm kit and stained with rabbit monoclonal PE-conjugated anti-activated caspase 3 antibody, per the manufacturer's protocol (BD Biosciences Pharmingen).

#### *CFU-F culture*

Bone marrow was isolated from mice treated 5 days with G-CSF and untreated controls. Nucleated cells (3.6 million) were plated per well in 6-well plates. Cells were grown for 4 days in  $\alpha$ MEM (Gibco) supplemented with 10% FBS and Pen/Strep. After 4 days, growth medium was switched to differentiation medium containing 50 mg/liter ascorbic acid and 2.16 mg/liter  $\beta$ -glycerophosphate (Sigma), and medium was changed every 3–4 days thereafter. After 14-day culture, cells were assayed for alkaline phosphatase (ALP) positivity using a kit (Sigma), and colonies containing >20 cells were scored.

#### *Bone marrow transplantation*

Wildtype (Ly5.1) and G-CSFR<sup>-/-</sup> (Ly5.2) bone marrow cells were harvested from strain- and sex-matched mice. Cells were stained with PE-conjugated mouse anti-CD45.1 or anti-CD45.2, APC-conjugated mouse anti-c-Kit, and FITC-conjugated lineage markers anti-CD3, anti-GR1, anti-B220, and anti-Ter119 antibodies. CD45<sup>+</sup>, c-Kit<sup>+</sup>, lineage<sup>-</sup> hematopoietic progenitors were purified by high-speed cell sorting, and 30,000–50,000 cells were injected into the tail vein of each lethally irradiated wildtype (Ly5.1) or G-CSFR<sup>-/-</sup> (Ly5.2) recipient as previously described.<sup>(15)</sup> Two independent groups of mice received transplants; mice were analyzed separately, and the results were pooled.

#### *Statistical analysis*

Data are presented as mean  $\pm$  SE. Statistical significance was assessed using the Mann-Whitney nonparametric test or two-way ANOVA (BrdU analysis).

## RESULTS

### *G-CSF treatment results in reduced numbers of osteoblasts but not osteocytes or bone-lining cells along bone surfaces*

We and others previously showed that treatment with G-CSF leads to fewer cuboidal osteoblasts from the bone marrow in mice.<sup>(9,10)</sup> To further characterize this process, we first determined the kinetics of osteoblast suppression during G-CSF treatment. As shown in Fig. 1A, reduced numbers of mature osteoblasts, as defined by histomorphological criteria, was delayed, with a significant fall seen after

3 days of G-CSF. This effect was reversible, because osteoblast number recovered within 5 days after stopping G-CSF.

These data were confirmed using transgenic mice expressing GFP driven by a 2.3-kb fragment of the rat type 1 collagen promoter (pOBCol2.3-GFP mice). Consistent with previous reports,<sup>(11,16)</sup> we observed GFP expression in these mice in mature, cuboidal osteoblasts, morphologically flat bone-lining cells, and osteocytes (Fig. 1B). G-CSF treatment resulted in fewer GFP<sup>+</sup> osteoblasts in trabecular and cortical bone. In contrast, G-CSF had no significant effect on the number of GFP<sup>+</sup> bone-lining cells or osteocytes (Figs. 1B and 1C).

We next developed a method to analyze and sort GFP<sup>+</sup> osteoblast lineage cells by flow cytometry. Briefly, hematopoietic and stromal cells were recovered from long bones by serial collagenase digestion. Immunohistochemistry performed on long bones after harvesting showed efficient recovery of GFP<sup>+</sup> cells from both control and G-CSF-treated mice (data not shown). Osteoblast lineage cells were defined as CD45<sup>-</sup> Ter119<sup>-</sup> GFP<sup>+</sup> cells; CD45<sup>+</sup> and Ter119<sup>+</sup> cells were excluded to improve specificity. Consistent with the histomorphometry data, this flow cytometry-based assay showed that the number of osteoblast lineage cells decreased after G-CSF administration (Figs. 1D and 1E).

### *G-CSF treatment selectively suppresses endosteal and trabecular but not periosteal osteoblasts*

To directly assess the effect of G-CSF treatment on bone formation, two functional assays of osteoblast activity were measured. Consistent with the loss of mature osteoblasts, a trend toward decreased osteoid synthesis ( $p = .057$ ) was observed in tibias of mice treated with G-CSF (Fig. 2A). Similarly, a trend toward decreased mineral apposition rate (MAR) and percent mineralized surface (Md.S/BS) was noted on the endosteal surfaces of calvaria harvested from G-CSF-treated mice ( $p = 0.10$ ; Fig. 2B). However, G-CSF had no effect on either parameter on the periosteal surfaces of calvaria. To test whether G-CSF treatment preferentially targets endosteal and trabecular osteoblasts in mouse long bones as well, we performed RNA in situ hybridization for osteocalcin mRNA. In untreated mice, osteocalcin mRNA was readily detected on endosteal, trabecular, and periosteal surfaces (Fig. 2C, left). As expected, G-CSF treatment resulted in a significant reduction in osteocalcin mRNA expression in endosteal and trabecular osteoblasts. In contrast, no significant decrease in osteocalcin expression in periosteal osteoblasts after G-CSF treatment was observed (Fig. 2C, center). Collectively, these data suggest that G-CSF selectively suppresses endosteal and trabecular osteoblasts.

### *G-CSF treatment suppresses osteoblast function through a hematopoietic cell intermediate*

The selective targeting of endosteal and trabecular osteoblasts by G-CSF suggested the hypothesis that its effects on osteoblasts are mediated by a hematopoietic cell intermediary. To test this hypothesis, bone marrow chimeras were generated by transplanting G-CSFR-deficient bone marrow



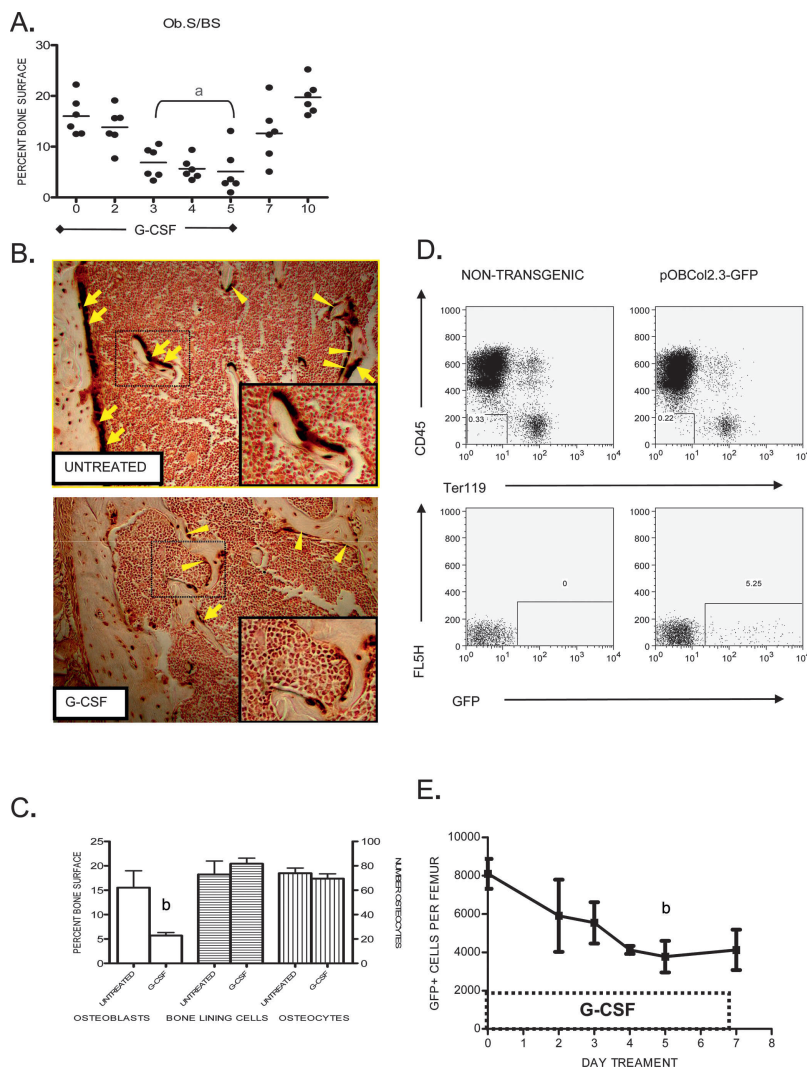


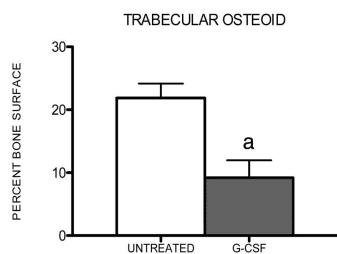
**FIG. 1.** Loss of osteoblast number and function during G-CSF treatment. (A) Mice were treated with G-CSF (250  $\mu\text{g}/\text{kg}/\text{d}$ ) for 5 days, and osteoblast surface per bone surface (Ob.S/BS) was determined. (B) Immunohistochemistry showing GFP<sup>+</sup> (brown) osteoblasts (arrows), bone-lining cells (arrowheads), and osteocytes in untreated or day 5 G-CSF treated pOBCol2.3-GFP transgenic mouse femurs. Insets show enlargement of area enclosed by dotted line. Original magnification  $\times 100$ . (C) Quantification of mature osteoblasts, bone-lining cells, and osteocytes in transgenic mice treated with G-CSF for 5 days or untreated ( $n = 4$  each group). (D) Representative scatter plots showing GFP expression (bottom panels) in the stromal (CD45 negative, Ter119 negative) cell population (top panels) isolated from nontransgenic and pOBCol2.3-GFP mice (left and right, respectively). (E) Number of GFP<sup>+</sup> cells recovered from the femurs of transgenic mice after treatment with G-CSF ( $n = 2$ –10 each time point). Data represent the mean  $\pm$  SE. <sup>a</sup> $p < 0.01$  vs. all other groups; <sup>b</sup> $p < 0.05$ .

cells into wildtype mice. Likewise, chimeras were generated in which wildtype bone marrow was transplanted into G-CSFR-deficient recipients. Because there is evidence suggesting that mesenchymal (stromal) cells can be transplanted to recipient mice,<sup>(16)</sup> we sorted hematopoietic progenitor cells (CD45<sup>+</sup> Kit<sup>+</sup> lineage<sup>-</sup>) to high purity before transplantation. Greater than 95% hematopoietic reconstitution with donor cells was confirmed in all chimeras 6–8 wk after transplantation (data not shown). Chimeric mice were treated 5 days with G-CSF, and the level of bone marrow osteocalcin mRNA was measured to gauge the effect of G-CSF on the osteoblast compartment. In chimeric mice reconstituted with G-CSFR-deficient hematopoietic cells, G-CSF treatment had no effect on osteocalcin expression (Fig. 3A). In contrast, G-CSF treatment induced a >30-fold decrease in osteocalcin mRNA in G-CSFR-deficient mice reconstituted with wildtype hematopoietic cells (Fig. 3B). These data show that G-CSF does not act directly on osteoblasts or other stromal cells. Instead, G-CSF suppresses osteoblasts through activation of a (presumably G-CSFR<sup>+</sup>) hematopoietic cell intermediate.

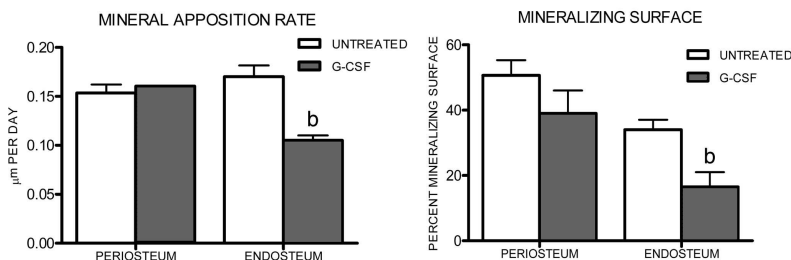
#### *G-CSF treatment increases osteoblast turnover by inducing apoptosis*

The decreased numbers of mature osteoblasts during G-CSF administration could occur through three general mechanisms: increased osteoblast turnover, decreased osteoblast production, or induction of osteoblast quiescence (with attendant loss of GFP expression from the type I collagen promoter). To begin to distinguish between these possibilities, we designed an experiment to measure the turnover rate of labeled osteoblast lineage cells. pOBCol2.3-GFP mice were treated with BrdU for 14 days before treatment with G-CSF. This treatment resulted in 32% of osteoblast lineage (GFP<sup>+</sup>) cells being labeled with BrdU (Fig. 4A). Mice were then treated with G-CSF, and the percentage of BrdU-labeled osteoblast lineage cells in the bone was determined as a function of time (Fig. 4A). In control mice, a gradual loss of BrdU<sup>+</sup> GFP<sup>+</sup> cells was observed, with a calculated half-life of 7.7 days. In mice treated with G-CSF, a more rapid turnover of BrdU<sup>+</sup> GFP<sup>+</sup> cells was observed, with a half-life of 3.7 days. Of note, after stopping G-CSF,

A.



B.



C.

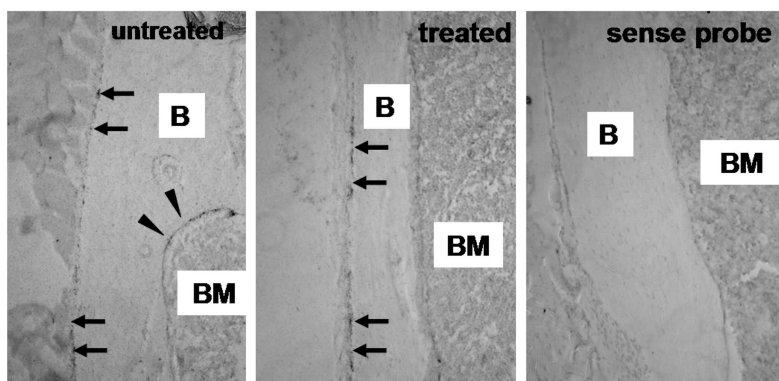


**FIG. 2.** Loss of endosteal and trabecular, but not periosteal, osteoblast activity during G-CSF treatment. Osteoid and mineralization were measured in untreated mice or mice treated for 7 days with G-CSF ( $n = 2-3$  each group). (A) Percent osteoid surface was calculated in Masson trichrome-stained tibial sections from untreated and treated wildtype mice. (B) Mineral apposition rate (MAR) and percent mineralizing surface (Mds/BS) were calculated on endosteal and periosteal surfaces from calcein-labeled calvaria. (C) Osteocalcin RNA in situ hybridization of long bones harvested from untreated mice or mice treated for 5 days with G-CSF. Shown are representative photomicrographs of three independent experiments. Periosteal surfaces (arrows), endosteal surfaces (arrowheads), bone (B), and bone marrow (BM) are indicated. Original magnification  $\times 100$ . Data represent the mean  $\pm$  SE. <sup>a</sup> $p = 0.057$ ; <sup>b</sup> $p = 0.10$ .

the turnover rate of BrdU<sup>+</sup> GFP<sup>+</sup> cells was similar in both groups of mice.

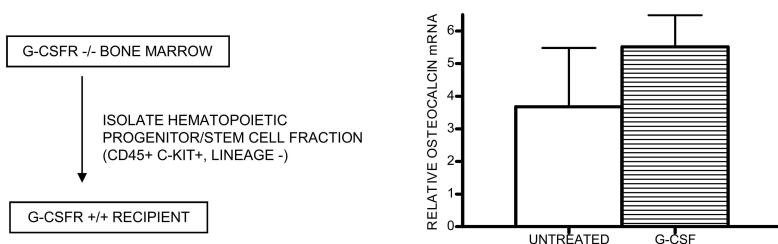
The increased turnover of osteoblasts after G-CSF administration suggested that G-CSF may induce osteoblast apoptosis. Indeed, regulation of osteoblast survival is thought to be an important mechanism regulating osteoblast number.<sup>(17)</sup> To test this hypothesis, we determined whether G-CSF treatment induced apoptosis of osteoblasts. Based on the kinetics of the decline in osteoblast numbers, we focused our analyses on day 3 of G-CSF treatment. GFP<sup>+</sup> osteoblast lineage cells were isolated from mice treated 3 days with G-CSF, and the percentage of GFP<sup>+</sup> cells expressing activated caspase 3 was determined by flow cytometry (Fig. 4B). In control mice,  $4.3 \pm 1.1\%$  of GFP<sup>+</sup> cells were apoptotic, as measured by activated caspase 3 expression. Of note, this number is within the range of reported values for osteoblast apoptosis in untreated mice.<sup>(18-22)</sup> In G-CSF-treated mice, the percentage of apoptotic cells was significantly increased ( $9.2 \pm 0.6\%$ ,  $p = 0.01$ ). These data suggest that G-CSF treatment suppresses mature osteoblasts, in least in part, by inducing apoptosis.

#### *G-CSF administration is associated with the inhibition of osteoblast differentiation*

We next asked whether osteoblast differentiation also was impaired after G-CSF administration. We first measured the effect of G-CSF on the expression of a panel of genes expressed at different stages of osteoblast differentiation (Fig. 5A). G-CSF treatment resulted in a significant decrease in all of the osteoblast genes analyzed. However, the greatest decrease in expression was observed with genes expressed late during osteoblast maturation. Whereas a 19-fold decrease in the late osteoblast gene *Bglap2* (OC) was observed, only a 1.8-fold reduction in the pan-osteoblast lineage transcription factor *Runx2* was noted.

The relative preservation of early osteoblast gene expression prompted us to examine the effect of G-CSF on osteoblast progenitor cells in the bone marrow. Specifically, the number of early mesenchymal colony forming unit-fibroblast (CFU-F) was measured. Both ALP<sup>+</sup>- and ALP<sup>-</sup>-staining colonies were enumerated. G-CSF treatment resulted in a 4.4-fold increase in ALP<sup>-</sup> and a 12.6-fold

A.



B.

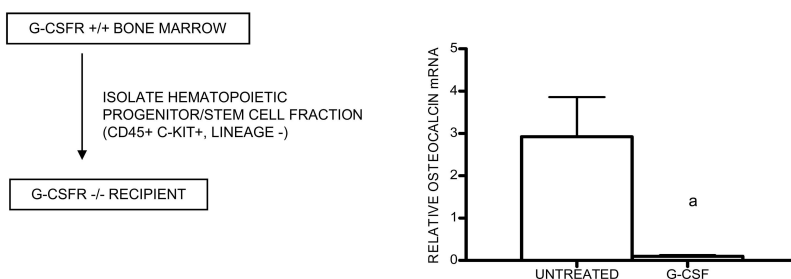


**FIG. 3.** G-CSF receptor-deficient bone marrow chimeras. (A) G-CSFR<sup>-/-</sup> CD45<sup>+</sup> cKit<sup>+</sup> lineage<sup>-</sup> hematopoietic cells (KL) cells were transplanted into wildtype recipients ( $n = 4-5$  each group). After hematopoietic reconstitution (6–8 wk), chimeric mice were treated with G-CSF (or left untreated), and osteocalcin mRNA expression in the bone marrow was measured by real-time RT-PCR. (B) Wildtype KL cells were transplanted into irradiated G-CSFR<sup>-/-</sup> recipients ( $n = 6-7$ , each group) and analyzed in a similar fashion. Data represent the mean  $\pm$  SE. <sup>a</sup> $p < 0.05$ .

increase in ALP<sup>+</sup> CFU-F over untreated controls (Fig. 5B). To determine whether this increase in osteoprogenitors resulted in a later increase in mature osteoblasts, we extended the period of G-CSF administration to 22 days and measured osteocalcin mRNA expression in the bone marrow (Fig. 5C). The decrease in osteocalcin mRNA expression was maximal by 5 days of G-CSF treatment and remained suppressed throughout the 22-day treatment period. Decreased osteoblast number was confirmed by histology (data not shown). The prolonged decrease in osteocalcin-producing osteoblasts, despite the increase in osteoprogenitors, suggests that G-CSF administration leads to a defect in osteoblast maturation in mice.

As noted previously, a prior study suggested that G-CSF treatment might induce osteoblast quiescence. This model predicts that the recovery of mature osteoblasts on discontinuation of G-CSF results from the reactivation of quiescent osteoblasts, rather than the production of new osteoblasts. To test this prediction, we measured BrdU uptake by osteoblasts during the recovery period after a 5-day course of G-CSF. In control mice,  $11.5 \pm 2.6\%$  of GFP<sup>+</sup> osteoblast lineage cells were labeled with BrdU at the end of the recovery phase, reflecting the rate of recruitment of new osteoblasts during this 5-day period (Fig. 5D). In contrast,  $31.3 \pm 3.6\%$  of GFP<sup>+</sup> cells were labeled in mice that had received G-CSF, indicating that the rebound in osteoblast number during the recovery phase results from recruitment of new osteoblasts rather than recovery of quiescent osteoblasts.

#### *G-CSF administration results in a decreased OPG/RANKL ratio and is associated with a late increase in osteoclast number*

Previous studies have established that chronic treatment with G-CSF leads to increased osteoclast number and activity.<sup>(4-6,23,24)</sup> Although there is evidence that G-CSF can directly activate the osteoclast lineage,<sup>(8)</sup> the potent suppressive effect of G-CSF on osteoblasts suggests another possibility. Namely, because osteoblasts contribute to the regulation of osteoclastogenesis, the reduced number of osteoblasts during G-CSF treatment may secondarily activate osteoclasts. Indeed, the kinetics of the decline in osteoblasts and increase in osteoclasts is consistent with this possibility. Whereas the decrease in osteoblast number was maximal after 5 days of G-CSF treatment (Fig. 1A), no increase in osteoclast number at this time point was noted, a result consistent with previous reports (Figs. 6A and 6B).<sup>(6,8)</sup> In fact, a significant increase in osteoclasts was not noted until after 14 days of G-CSF treatment.

A major mechanism by which osteoblasts regulate osteoclast number and activity is by the regulated production of RANKL (*TNFSF11*) and OPG (*TNFRSF11B*), a decoy receptor for RANKL. RANKL and OPG are positive and negative regulators of osteoclasts, respectively; thus, the relative expression of these genes is a key determinant of osteoclast activation.<sup>(25)</sup> In mice treated with G-CSF for 5 days, no change in RANKL mRNA expression in the bone marrow was detected (Fig. 6C). In contrast, a 12-fold de-

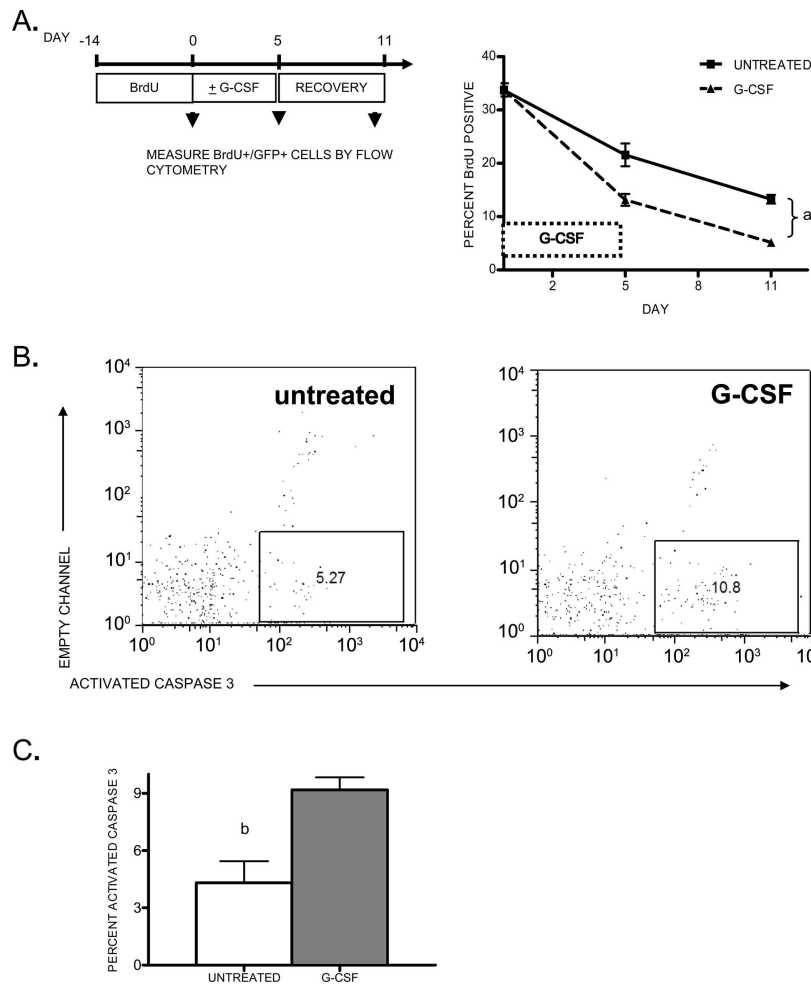


**FIG. 4.** Osteoblast turnover during G-CSF treatment. (A) Transgenic pOBCol2.3-GFP mice ( $n = 5-6$ , each group) were administered BrdU for 14 days and either treated for 5 days with G-CSF or left untreated. Mice were analyzed just before G-CSF treatment, after 5 days of G-CSF treatment, or after a 5 day recovery period (arrowheads). Shown is the percent of GFP<sup>+</sup> cells in the bone marrow that were labeled with BrdU. (B) Representative scatter plots showing activated caspase 3 staining in the GFP<sup>+</sup> cell population from untreated (left) or G-CSF-treated pOBCol2.3-GFP mice (right). (C) Shown is the percentage of GFP<sup>+</sup> cells that express activated caspase 3 from untreated and day 3 G-CSF-treated mice ( $n = 4$  each group). Data represent the mean  $\pm$  SE. <sup>a</sup> $p < 0.01$ , <sup>b</sup> $p < 0.05$ .

crease in OPG mRNA was observed after 5 days of G-CSF treatment (Fig. 6C). The ratio of RANKL to OPG mRNA increased from 0.19 at baseline to 1.98 after 14 days of G-CSF. To verify that the loss of OPG mRNA resulted from the loss of osteoblasts, pOBCol2.3-GFP transgenic mice were treated with G-CSF, GFP<sup>+</sup> osteoblast-lineage cells were isolated, and OPG and RANKL mRNA was measured. Whereas RANKL expression was preserved within this fraction after G-CSF treatment, OPG mRNA was reduced 10-fold, consistent with the reduction in GFP<sup>+</sup> mature osteoblasts (Fig. 6D).

## DISCUSSION

In this study, we confirmed and extended our previous finding that G-CSF treatment suppresses osteoblast number and activity. This effect seems to be specific to mature osteoblasts, because other osteoblast-lineage cells, including osteocytes and bone-lining cells, are unperturbed. We provide evidence that G-CSF treatment increases apoptosis of mature osteoblasts while increasing the numbers of osteoprogenitors in the bone marrow. Transplantation experiments show that G-CSF regulates osteoblasts in an indirect fashion through activation of an undetermined hematopoi-

etic cell intermediary. Finally, we show that G-CSF treatment significantly alters the relative expression of RANKL and OPG in the bone marrow, providing a novel mechanism by which G-CSF treatment results in osteoclast activation.

Apoptosis is thought to be one of the primary regulators of osteoblast homeostasis. There is evidence that glucocorticoid treatment and estrogen withdrawal suppress osteoblast number through the induction of apoptosis.<sup>(22,26)</sup> Conversely, inhibition of osteoblast apoptosis during intermittent parathyroid treatment may contribute to the bone anabolic effect seen with this treatment.<sup>(21)</sup> In this study, we showed that G-CSF treatment results in an ~2-fold increase in the turnover rate of BrdU-labeled osteoblast lineage cells in the bones of treated animals. Moreover, the percentage of cleaved caspase 3-positive osteoblasts recovered from G-CSF-treated mice was increased 2-fold compared with control mice. Together, these data suggest that G-CSF regulates osteoblast number, in part by, inducing osteoblast apoptosis.

The following observations suggest that G-CSF also inhibits osteoblast differentiation *in vivo*. (1) G-CSF administration results in a marked increase in osteoprogenitors. (2) The increase in osteoprogenitors does not “rescue” the



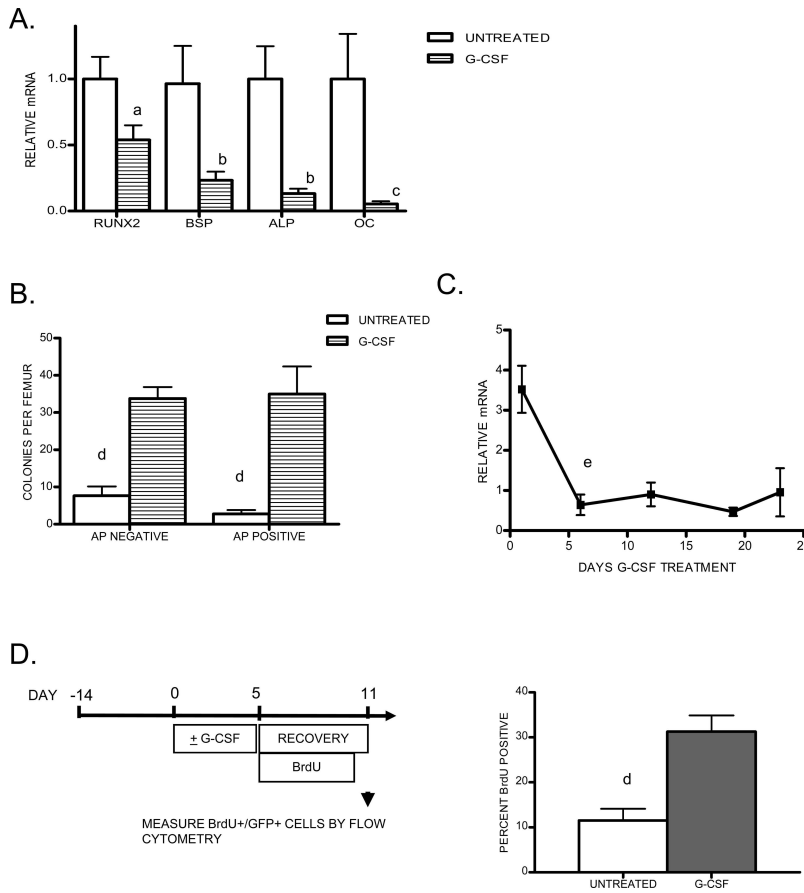


**FIG. 5.** Analysis of early osteoblast lineage cells during G-CSF treatment. (A) Real-time RT-PCR for the indicated genes (BSP, bone sialoprotein; ALP, alkaline phosphatase; OC, osteocalcin) was performed on total bone marrow RNA isolated after 5 days of G-CSF treatment. RNA expression relative to  $\beta$ -actin mRNA was calculated and compared with untreated bone marrow (assigned a value of 1;  $n = 5-12$ ). (B) Shown is the number of alkaline phosphatase negative (AP negative, left) and positive (AP positive, right) CFU-F generated from the bone marrow of untreated or G-CSF-treated mice ( $n = 5-6$  each group). (C) Mice ( $n = 2-4$  each time point) were treated with G-CSF for the indicated period up to 22 days. Mice were killed at the indicated time points and analyzed for osteocalcin mRNA by real-time RT-PCR. (D) Mice ( $n = 6$ , each group) were treated 5 days with G-CSF or left untreated and administered BrdU for 5 days during the recovery period. Shown is the percent of GFP<sup>+</sup> cells in the bone marrow that were labeled with BrdU. Data represent the mean  $\pm$  SE. <sup>a</sup>*p* < 0.05 vs. untreated; <sup>b</sup>*p* < 0.01 vs. untreated, *p* < 0.05 vs. runx2 and OC; <sup>c</sup>*p* < 0.0001 vs. untreated, *p* < 0.05 vs. other groups; <sup>d</sup>*p* < 0.01; <sup>e</sup>*p* < 0.05 vs. untreated.

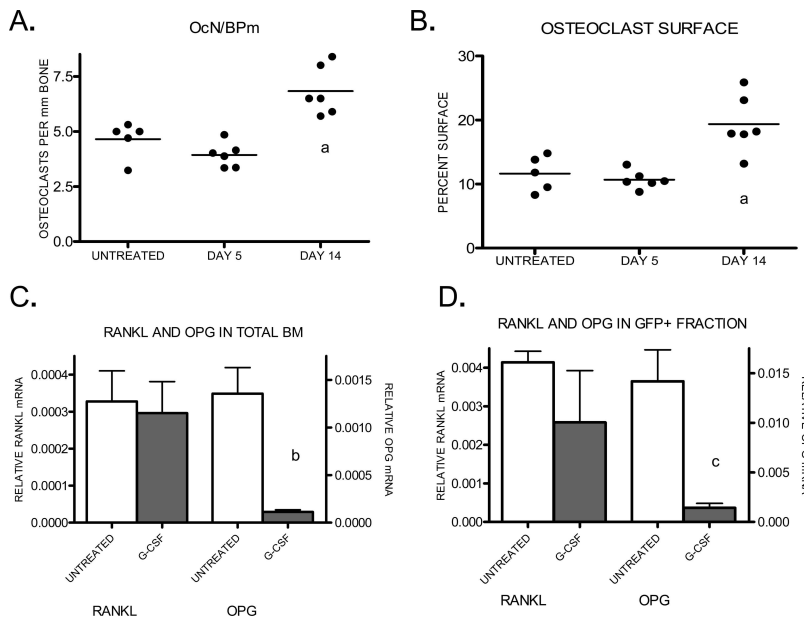


**FIG. 6.** Osteoclastogenesis during G-CSF treatment. (A and B) Wildtype mice ( $n = 2-6$  each group) were treated with G-CSF for the indicated time or left untreated. Osteoclast number (A) and surface (B) were estimated by enumerating TRACP<sup>+</sup> cells in paraffin-embedded sections of mouse long bones. (C) RANKL and OPG mRNA expression in the bone marrow of untreated or 5-day G-CSF-treated mice ( $N = 5-8$  each group) was measured by real-time RT-PCR. (D) GFP<sup>+</sup> cells were sorted from G-CSF-treated pOBCol2.3-GFP mice. RANKL and OPG mRNA was measured within this fraction. Data represent the mean  $\pm$  SE. <sup>a</sup>*p* < 0.01 vs. other groups; <sup>b</sup>*p* < 0.001; <sup>c</sup>*p* < 0.05.

defect in mature osteoblasts, even after prolonged (22 days) G-CSF administration. In contrast, the increase in osteoprogenitors observed after estrogen withdrawal, which induces a greater degree of osteoblast apoptosis, is able to restore osteoblast number to normal.<sup>(27,28)</sup> (3) Expression

of genes associated with earlier stages of osteoblast differentiation (e.g., *Runx2*) is reduced less than genes associated with later stages (e.g., *Bglap2*). (4) Finally, the rapid recovery of osteoblasts with proliferating (BrdU-labeled) cells after cessation of G-CSF suggests that G-CSF administration



leads to the accumulation of an expanded pool of osteoblast precursors in the bone marrow. Collectively, these data suggest G-CSF administration leads to a reduction in number of mature osteoblasts through both an increase in osteoblast turnover and inhibition of osteoblast differentiation.

In addition to hematopoietic cells, there is data suggesting that the G-CSFR is expressed on wide range of nonhematopoietic tissues including endothelial cells, neurons, and possibly cardiomyocytes.<sup>(29,30)</sup> Previous studies have shown that the G-CSFR is not expressed on osteoblast cells lines or cultured primary murine calvarial osteoblasts.<sup>(9,10)</sup> Whether the G-CSFR is expressed on osteoblasts *in vivo* has not been determined; therefore, the possibility that G-CSF's effects on osteoblasts are direct cannot be excluded. In this study, we provide definitive evidence through the use of G-CSFR-deficient bone marrow chimeras that G-CSF acts indirectly to suppress osteoblasts. Indeed, these data strongly suggest that this phenotype is dependent on a transplantable hematopoietic cell intermediate. Consistent with this conclusion, G-CSF treatment preferentially targets endosteal and trabecular osteoblasts, with little effect on periosteal osteoblasts.

The hematopoietic cell population(s) that mediate the suppressive effect of G-CSF on osteoblasts are not known. The G-CSFR is expressed at high levels on neutrophils, monocytes, osteoclasts, and hematopoietic progenitors. There also are reports of G-CSFR expression on natural killer cells and a subset of B lymphocytes. However, the suppressive effect of G-CSF treatment on osteoblasts is preserved in *RAG1*-deficient mice, suggesting that lymphocytes are not required for this effect.<sup>(9)</sup> Studies are underway to define the role of neutrophils, monocytes, and osteoclasts in this pathway.

The pathway leading from hematopoietic cell activation by G-CSF to osteoblast apoptosis also remains poorly understood. In a series of elegant studies, Katayama et al.<sup>(9)</sup> recently provided evidence that G-CSF-induced osteoblast suppression is mediated by the sympathetic nervous system. Our studies of G-CSFR-deficient bone marrow chimeras strongly suggest that G-CSF does not act directly on neurons to suppress osteoblasts. Rather, our data raise the possibility that G-CSF-induced activation of hematopoietic cells indirectly leads to activation of the sympathetic nervous system and ultimately osteoblast apoptosis.

A consistent feature of G-CSF-induced osteopenia in both humans and mice is osteoclast activation. Previous studies have shown that G-CSF can act directly on osteoclast precursors stimulating their differentiation *in vitro* into mature osteoclasts.<sup>(8)</sup> In this study, we provide evidence for a novel mechanism by which G-CSF treatment leads to osteoclast activation. G-CSF treatment leads to a marked decrease in OPG expression in the bone marrow, whereas levels of RANKL expression remain relatively constant. This altered ratio of OPG to RANKL expression is predicted to increase RANK signaling in osteoclast precursors, thereby stimulating osteoclast production and activation. In addition to osteoblasts, RANKL and OPG are also expressed by other stromal cells and certain lymphocyte subsets.<sup>(25)</sup> However, our data suggest that G-CSF specifically targets the osteoblast lineage, because OPG ex-

pression was markedly decreased after G-CSF administration in sorted GFP<sup>+</sup> cells from pOBCol2.3-GFP transgenic mice. Consistent with this conclusion, G-CSF-dependent osteoclastogenesis was not observed until at least 5 days after the beginning of G-CSF treatment, at which time the G-CSF-induced decline in osteoblasts was complete. This late activation of osteoclasts by G-CSF corroborates reports from other groups<sup>(6,8)</sup> and supports the notion that loss of OPG expression plays an important role in stimulating osteoclastogenesis during G-CSF treatment *in vivo*.

In summary, G-CSF signaling through hematopoietic cells in the bone marrow exerts powerful effects on both osteoblasts and osteoclasts, resulting in imbalance between bone formation and resorption. It is hoped that by continuing to unravel the pathways by which G-CSF targets bone cells, greater insight will be gained into how the hematopoietic compartment interacts with bone cells.

## ACKNOWLEDGMENTS

The authors thank David J Rowe for providing the pOBCol2.3-GFP mice, Amgen for providing the G-CSF, and Deborah V Novack for assistance with the histomorphometric analysis. We also thank Deborah V Novack, Roberto Civitelli, and F Patrick Ross for critical review of this manuscript. This work was supported by a National Institutes of Health Grant HL60772.

## REFERENCES

1. Taichman RS 2005 Blood and bone: Two tissues whose fates are intertwined to create the hematopoietic stem-cell niche. *Blood* **105**:2631–2639.
2. Lorenzo J 2000 Interactions between immune and bone cells: New insights with many remaining questions. *J Clin Invest* **106**:749–752.
3. Dale DC, Cottle TE, Fier CJ, Bolyard AA, Bonilla MA, Boxer LA, Cham B, Freedman MH, Kannourakis G, Kinsey SE, Davis R, Scarlata D, Schwinzer B, Zeidler C, Welte K 2003 Severe chronic neutropenia: Treatment and follow-up of patients in the Severe Chronic Neutropenia International Registry. *Am J Hematol* **72**:82–93.
4. Lee MY, Fukunaga R, Lee TJ, Lottsfeldt JL, Nagata S 1991 Bone modulation in sustained hematopoietic stimulation in mice. *Blood* **77**:2135–2141.
5. Takahashi T, Wada T, Mori M, Kokai Y, Ishii S 1996 Overexpression of the granulocyte colony-stimulating factor gene leads to osteoporosis in mice. *Lab Invest* **74**:827–834.
6. Takamatsu Y, Simmons PJ, Moore RJ, Morris HA, To LB, Levesque JP 1998 Osteoclast-mediated bone resorption is stimulated during short-term administration of granulocyte colony-stimulating factor but is not responsible for hematopoietic progenitor cell mobilization. *Blood* **92**:3465–3473.
7. Purton LE, Lee MY, Torok-Storb B 1996 Normal human peripheral blood mononuclear cells mobilized with granulocyte colony-stimulating factor have increased osteoclastogenic potential compared to nonmobilized blood. *Blood* **87**:1802–1808.
8. Hirbe AC, Uluckan O, Morgan EA, Eagleton MC, Prior JL, Pivnicka-Worms D, Trinkaus K, Apicelli A, Weilbaecher K 2006 Granulocyte colony-stimulating factor enhances bone tumor growth in mice in an osteoclast-dependent manner. *Blood* **109**:3424–3431.
9. Katayama Y, Battista M, Kao WM, Hidalgo A, Peired AJ, Thomas SA, Frenette PS 2006 Signals from the sympathetic nervous system regulate hematopoietic stem cell egress from bone marrow. *Cell* **124**:407–421.

10. Semerad CL, Christopher MJ, Liu F, Short B, Simmons PJ, Winkler I, Levesque JP, Chappel J, Ross FP, Link DC 2005 G-CSF potently inhibits osteoblast activity and CXCL12 mRNA expression in the bone marrow. *Blood* **106**:3020–3027.
11. Kalajzic Z, Liu P, Kalajzic I, Du Z, Braut A, Mina M, Canalis E, Rowe DW 2002 Directing the expression of a green fluorescent protein transgene in differentiated osteoblasts: Comparison between rat type I collagen and rat osteocalcin promoters. *Bone* **31**:654–660.
12. Liu F, Wu HY, Wesselschmidt R, Kornaga T, Link DC 1996 Impaired Production and Increased Apoptosis of Neutrophils in Granulocyte Colony-Stimulating Factor Receptor-Deficient Mice. *Immunity* **5**:491–501.
13. Castro CH, Shin CS, Stains JP, Cheng SL, Sheikh S, Mbalaviele G, Szejnfeld VL, Civitelli R 2004 Targeted expression of a dominant-negative N-cadherin in vivo delays peak bone mass and increases adipogenesis. *J Cell Sci* **117**:2853–2864.
14. Xu J, Lawshe A, MacArthur CA, Ornitz DM 1999 Genomic structure, mapping, activity and expression of fibroblast growth factor 17. *Mech Dev* **83**:165–178.
15. Richards MK, Liu F, Iwasaki H, Akashi K, Link DC 2003 Pivotal role of granulocyte colony-stimulating factor in the development of progenitors in the common myeloid pathway. *Blood* **102**:3562–3568.
16. Wang L, Liu Y, Kalajzic Z, Jiang X, Rowe DW 2005 Heterogeneity of engrafted bone-lining cells after systemic and local transplantation. *Blood* **106**:3650–3657.
17. Jilka RL 2003 Biology of the basic multicellular unit and the pathophysiology of osteoporosis. *Med Pediatr Oncol* **41**:182–185.
18. Pereira RC, Stadmeier LE, Smith DL, Rydzziel S, Canalis E 2007 CCAAT/Enhancer-binding protein homologous protein (CHOP) decreases bone formation and causes osteopenia. *Bone* **40**:619–626.
19. Sheng MH, Lau KH, Mohan S, Baylink DJ, Wergedal JE 2006 High osteoblastic activity in C3H/HeJ mice compared to C57BL/6J mice is associated with low apoptosis in C3H/HeJ osteoblasts. *Calcif Tissue Int* **78**:293–301.
20. Borton AJ, Frederick JP, Datto MB, Wang XF, Weinstein RS 2001 The loss of Smad3 results in a lower rate of bone formation and osteopenia through dysregulation of osteoblast differentiation and apoptosis. *J Bone Miner Res* **16**:1754–1764.
21. Jilka RL, Weinstein RS, Bellido T, Roberson P, Parfitt AM, Manolagas SC 1999 Increased bone formation by prevention of osteoblast apoptosis with parathyroid hormone. *J Clin Invest* **104**:439–446.
22. Weinstein RS, Jilka RL, Parfitt AM, Manolagas SC 1998 Inhibition of osteoblastogenesis and promotion of apoptosis of osteoblasts and osteocytes by glucocorticoids. Potential mechanisms of their deleterious effects on bone. *J Clin Invest* **102**:274–282.
23. Fewtrell MS, Kinsey SE, Williams DM, Bishop NJ 1997 Bone mineralization and turnover in children with congenital neutropenia, and its relationship to treatment with recombinant human granulocyte-colony stimulating factor. *Br J Haematol* **97**:734–736.
24. Yakisan ESE, Zeidler C, Bishop NJ, Reiter A, Hirt A, Riehm H, Welte K 1997 Oct;131(4):592-7. High incidence of significant bone loss in patients with severe congenital neutropenia (Kostmann's syndrome). *J Pediatr* **131**:592–597.
25. Theoleyre S, Wittrant Y, Tat SK, Fortun Y, Redini F, Heymann D 2004 The molecular triad OPG/RANK/RANKL: Involvement in the orchestration of pathophysiological bone remodeling. *Cytokine Growth Factor Rev* **15**:457–475.
26. Kousteni S, Bellido T, Plotkin LI, O'Brien CA, Bodenner DL, Han L, Han K, DiGregorio GB, Katzenellenbogen JA, Katzenellenbogen BS, Roberson PK, Weinstein RS, Jilka RL, Manolagas SC 2001 Nongenotropic, sex-nonspecific signaling through the estrogen or androgen receptors: Dissociation from transcriptional activity. *Cell* **104**:719–730.
27. Kousteni S, Chen JR, Bellido T, Han L, Ali AA, O'Brien CA, Plotkin L, Fu Q, Mancino AT, Wen Y, Vertino AM, Powers CC, Stewart SA, Ebert R, Parfitt AM, Weinstein RS, Jilka RL, Manolagas SC 2002 Reversal of bone loss in mice by nongenotropic signaling of sex steroids. *Science* **298**:843–846.
28. Jilka RL, Takahashi K, Munshi M, Williams DC, Roberson PK, Manolagas SC 1998 Loss of estrogen upregulates osteoblastogenesis in the murine bone marrow. Evidence for autonomy from factors released during bone resorption. *J Clin Invest* **101**:1942–1950.
29. Jung KH, Chu K, Lee ST, Kim SJ, Sinn DI, Kim SU, Kim M, Roh JK 2006 Granulocyte colony-stimulating factor stimulates neurogenesis via vascular endothelial growth factor with STAT activation. *Brain Res* **1073-1074**:190–201.
30. Harada M, Qin Y, Takano H, Minamino T, Zou Y, Toko H, Ohtsuka M, Matsuura K, Sano M, Nishi J, Iwanaga K, Akazawa H, Kunieda T, Zhu W, Hasegawa H, Kunisada K, Nagai T, Nakaya H, Yamauchi-Takahara K, Komuro I 2005 G-CSF prevents cardiac remodeling after myocardial infarction by activating the Jak-Stat pathway in cardiomyocytes. *Nat Med* **11**:305–311.

Address reprint requests to:

*Daniel C Link, MD*

*Division of Oncology*

*Department of Medicine*

*660 South Euclid Avenue, Campus Box 8007*

*St Louis, MO 63110, USA*

*E-mail: dlink@im.wustl.edu*

Received in original form November 8, 2007; revised form June 20, 2008; accepted June 27, 2008.